Charge ordering in half-doped manganites

PHYSICAL REVIEW B **70**, 140404(R) (2004)

Charge ordering in half-doped manganites

R. J. Goff[1,2] and J. P. Attfield[1]

[1]*Centre for Science at Extreme Conditions, University of Edinburgh, Erskine, Williamson Building, King's Buildings, Mayfield Road, Edinburgh, EH9 3JZ, United Kingdom*

[2]*Department of Chemistry, University of Cambridge, Lensfield Road, Cambridge, CB2 1EW, United Kingdom*

(Received 16 August 2004; published 13 October 2004)

Alternative descriptions for the ground state structure of the half-doped manganite $Pr_{0.5}Ca_{0.5}MnO_3$ have been tested against high-resolution 10 K x-ray and neutron powder diffraction data. The best fit is obtained using a $P2_1/m$ symmetry model, which supports the striped charge and orbital ordering picture. The magnitude of the charge ordering is, however, only 25% of the ideal Mn^{3+}/Mn^{4+} separation. An alternative $Pnm2_1$ pseudosymmetry, used to describe Zener polaron ordering in $Pr_{0.6}Ca_{0.4}MnO_3$ [Phys. Rev. Lett. **89**, 097205 (2002)], gives a different, bistriped, charge and orbitally ordered model that does not fit the data as well.

DOI: 10.1103/PhysRevB.70.140404 PACS number(s): 75.47.Gk, 71.45.Lr, 61.66.Fn, 71.70.Ch

The physics of manganite perovskites has been studied intensively in recent years following the discovery of colossal magnetoresistances in many compositions based on doped $LaMnO_3$.[1] These materials show an unprecedented range of couplings between Mn spin, charge, and lattice degrees of freedom. It is now established that several ground states are possible for doped manganites, principally the itinerant ferromagnetic and insulating charge ordered antiferromagnetic states, and these often coexist over a range of length scales.[2]

The charge-ordered (CO) ground state is most easily observed in half-doped manganites such as $La_{0.5}Ca_{0.5}MnO_3$. The model for this CO phase was proposed by Goodenough[3] after the magnetic structure had been found to be the complex CE-type with ferromagnetic couplings along zigzag chains.[4] The model assumed that localized Mn^{3+} and Mn^{4+} states order in alternate planes ("stripes") as shown in Fig. 1. Orbital ordering (OO) results from the Jahn-Teller distortion of the high spin $3d^4$ Mn^{3+} configuration, and the resulting superexchange interactions are consistent with the observed CE-type spin structure.

A powder x-ray and neutron powder diffraction study of $La_{0.5}Ca_{0.5}MnO_3$ (Refs. 5 and 6) discovered an incommensurate $[\frac{1}{2}\text{-}\varepsilon,0,0]$ modulation of the common $\sqrt{2a_p}\times 2a_p \times \sqrt{2a_p}$ *Pnma* perovskite ($a_p \approx 3.8$ Å) superstructure. The *Pnma* superstructure contains only one symmetry-equivalent Mn site and so does not describe long-range CO. At low temperatures, ε tends to small values, which enabled the crystal structure to be refined in a monoclinic $P2_1/m$ symmetry $2\sqrt{2a_p}\times 2a_p \times \sqrt{2a_p}$ superstructure with two displacement coordinates to describe the charge and orbital ordering modulation of the *Pnma* structure. The results confirmed the striped CO model. The structures of several other half-doped manganites have subsequently been fitted using the same model,[7–9] allowing up to seven coordinate variables (for $Nd_{0.5}Sr_{0.5}MnO_3$) (Ref. 7) to describe the CO and OO modulations. However, a fully unconstrained refinement of the $P2_1/m$ model has not been reported.

An alternative refinement model for half-doped manganites has recently been derived from a neutron diffraction study of a single crystal of $Pr_{0.6}Ca_{0.4}MnO_3$.[10] (The 1:1 CO structure modulation is found for $0.3<x<0.5$ in $Pr_{1-x}Ca_xMnO_3$, implying substitution of Mn^{3+} at the Mn^{4+} sites for $x\neq 0.5$). This study showed that the $2\sqrt{2a_p}\times 2a_p \times \sqrt{2a_p}$ supercell has *Pm* monoclinic symmetry so that the four Mn sites shown in Fig. 1 are symmetry independent. Orthorhombic $Pnm2_1$ symmetry constraints were applied—this constrains sites 1a and 2a, and sites 1b and 2b, to be equivalent. No charge difference between the a and b sites was found, supporting a Zener polaron ordering (ZPO) model in which an electron is localized in Mn-O-Mn bridges by double exchange when the Mn spins are parallel, so the Mn sites both have an average valence of +3.5. Other results have suggested that ZPO or CO ground states occur in 50% doped manganites for different values of the perovskite tolerance factor,[11] or combine to form intermediate states for $0.4<x<0.5$.[12]

Solid state ^{17}O NMR spectra of $Pr_{0.5}Ca_{0.5}MnO_3$ (Ref. 13) did not conclusively discriminate between these two models, although the number of oxygen resonances was consistent with the striped CO picture, and suggested that some delocalization of the e_g electron occurs. Resonant Mn *K* edge x-ray diffraction studies on $Pr_{1-x}Ca_xMnO_3$ (Refs. 14 and 15), and $Nd_{0.5}Sr_{0.5}MnO_3$ (Ref. 16) have supported the striped CO model over the ZPO structure, although whether a full charge ordering is present has been debated.[17] Theoretical calculations have estimated that the magnitude of charge separation is 19% of the ideal Mn^{3+}/Mn^{4+} difference.[18]

We have tested both the striped CO and the ZPO models against highly resolved powder x-ray and neutron diffraction data collected at 10 K from a polycrystalline sample of $Pr_{0.5}Ca_{0.5}MnO_3$. Time-of-flight neutron diffraction data were collected from a 5 mm deep flat plate sample in 12 hours on diffractometer HRPD at the ISIS spallation source, United Kingdom. X-ray diffraction from a 0.4 mm capillary was measured for six hours on instrument ID31 at ESRF, Grenoble, up to a 2θ angle of 70° at a wavelength of 0.588878 Å. Each structural model was Rietveld-fitted to the backscattering neutron diffraction data (*d*-space range $d=0.8-2.1$ Å) and the x-ray data ($d=0.8-4.0$ Å) together using the GSAS software package.[19] Magnetic neutron diffraction from the CE-type arrangement was fitted with Mn moments parallel to the *z* axis.

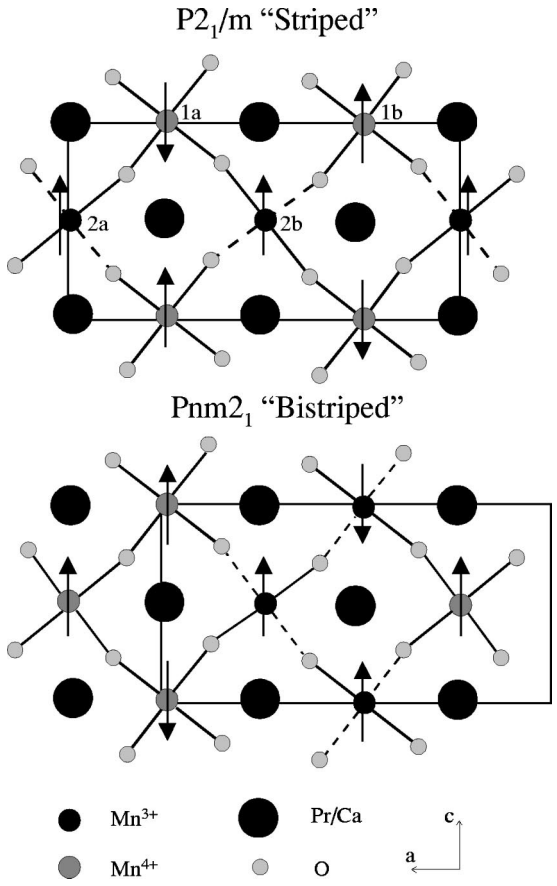

FIG. 1. The refined charge and orbitally ordered arrangements in $Pr_{0.5}Ca_{0.5}MnO_3$ using $P2_1/m$ or $Pnm2_1$ pseudosymmetries. The elongated Mn-O bonds at the Mn^{3+} sites corresponding to the d_{z^2} orbitals are shown as broken lines and the arrows show spin directions for a CE-type arrangement as consistent as possible with the orbital orderings. The Mn site labels are shown on the $P2_1/m$ model.

Rapid neutron diffraction scans at temperatures close to the CO transition (230 K) and longer scans at 180 K and 70 K revealed the temperature-dependent $[\frac{1}{2}\text{-}\varepsilon,0,0]$ modulation observed in other studies,[6] but at 10 K the incommensurability ε is negligible, enabling the structure to be refined on the monoclinic $2\sqrt{2}a_p \times 2a_p \times \sqrt{2}a_p$ supercell. No additional broadening of the superstructure reflections was observed. It was not possible to refine the crystal structure of $Pr_{0.5}Ca_{0.5}MnO_3$ against the combined neutron and x-ray data assuming space group Pm without symmetry constraints, due to the large number (67) of independent coordinates. However, convergent refinements were obtained by applying $P2_1/m$ or $Pnm2_1$ symmetry constraints to the atomic positions, which reduce the number of variable atomic coordinates to 33 or 31, respectively.[20] The final structural models were reproducible from several starting points and so are taken to be the true minima for the refinements. A comparison of the fitting indices, Mn-O bond lengths and Mn valences (calculated using the bond valence sum method[21]) is given in Table I.

The fitting indices for the two refinements show that the $P2_1/m$ and the $Pnm2_1$ models give equivalent fits to the x-ray data, but the fit to the neutron intensities [R_{F^2}(N) residuals in Table I] is significantly better with the $P2_1/m$ model. This is also evident by visual inspection of the neutron superstructure intensities that are sensitive to the different models, such as the $(h,k,l)=(\text{odd},\text{even},\text{odd})$ subset of reflections (Fig. 2) for which $R_{F^2}(\text{N})=10.5\%$ for the $P2_1/m$ model and 12.7% for the $Pnm2_1$ model. The higher fit quality of the $P2_1/m$ model leads us to conclude that this is a better description of the structure of $Pr_{0.5}Ca_{0.5}MnO_3$ than the $Pnm2_1$ refinement. The refined $P2_1/m$ structural parameters are given in Table II.

It is useful to compare the refined $P2_1/m$ and the $Pnm2_1$ models as both give charge and orbitally ordered descriptions for $Pr_{0.5}Ca_{0.5}MnO_3$. In $P2_1/m$ symmetry (Fig. 1), there are three independent Mn sites; 1(a and b), 2a, and 2b. The refined Mn-O distances and BVS estimates of formal charge (Table I) show that these sites approximate to Mn^{4+}, Mn^{3+}, and Mn^{3+}, respectively, with the latter sites showing elongation of one pair of bonds in the ac plane characteristic of OO. This is the striped picture for CO and OO;[3] however, the differences between the BVS values show that the CO is only 25% of the theoretical separation of one charge unit. This is in good agreement with the 19% charge separation estimated from theoretical calculations.[18]

In the $Pnm2_1$ description (Fig. 1), the refinement again evidences charge ordering of Mn^{4+} and Mn^{3+}, respectively, at the two independent Mn sites, (1 and 2)a and (1 and 2)b. The two sites are arranged in double rows and so this model describes a bistriped charge ordering, in contrast to the singly striped $P2_1/m$ model. OO distortions are seen in the double stripes of Mn^{3+} at the b sites, resulting in elongation of the $\pm(\frac{1}{2}\mathbf{a}-\mathbf{c})$ oriented Mn1b-O bonds (Table I). The distortion is less regular than in the $P2_1/m$ model because of the direct connections between Mn^{3+} octahedra in the bistripes. The BVS's for the two Mn sites are very similar to those in the $P2_1/m$ refinement. Hence, both the $P2_1/m$ and the $Pnm2_1$ refinements give physically plausible charge and orbitally ordered models for $Pr_{0.5}Ca_{0.5}MnO_3$, corresponding to striped and bistriped CO models, respectively.

Although the $Pnm2_1$ refinement model does not provide the best fit to the data, it nevertheless describes an alternative CO and OO model, whereas in the previous single crystal study of $Pr_{0.6}Ca_{0.4}MnO_3$, the same pseudosymmetry did not reveal any CO or OO at the two Mn sites. This discrepancy may arise from two factors. Although single crystal diffraction experiments generally give more precise structure refinements than powder methods, they are sensitive to crystal twinning which commonly results from the small lattice distortions that accompany CO. The single crystal data for $Pr_{0.6}Ca_{0.4}MnO_3$ were analyzed assuming six twin domains.[10] A second factor is the use of a 40% rather than a 50% doped manganite. Although a constant lattice periodicity is found for charge-ordered $Pr_{1-x}Ca_xMnO_3$ in the range $x=0.3-0.5$, the additional disorder introduced at $x=0.4$ (where 1 in 5 of the Mn^{4+} sites are occupied by Mn^{3+}) is likely to reduce the range and magnitude of the CO to below the practical limit of $\sim$10% observable by crystal structure refinement. It would be interesting to perform a high resolution powder diffraction study of $Pr_{0.6}Ca_{0.4}MnO_3$ for direct comparison with the present work.

TABLE I. A comparison of the refinement results for $Pr_{0.5}Ca_{0.5}MnO_3$ at 10 K using $Pnm2_1$ or $P2_1/m$ pseudosymmetry models. The fitting parameters are the overall reduced χ^2 and residuals for the x ray (X) and neutron (N) profiles. Mn-O distances are shown for the three pairs of bonds in the given directions (see Fig. 1) followed by the mean value and the bond valence sum (BVS) (Ref. 21) for each unique Mn site.

Model	$Pnm2_1$		$P2_1/m$		
χ^2	7.70		7.56		
$R_{wp}(N)$ (%)	5.52		4.95		
$R_{wp}(X)$ (%)	11.28		11.51		
$R_{F^2}(N)$ (%)	6.58		4.58		
$R_{F^2}(X)$ (%)	4.69		4.73		
Mn-O distances (Å)	Mn1a	Mn1b	Mn1a	Mn2a	Mn2b
$\pm\mathbf{b}$	1.985(6) 1.854(6)	1.909(7) 1.908(7)	1.977(5) 1.851(5)	1.907(3) (×2)	1.922(3) (×2)
$\pm(\frac{1}{2}\mathbf{a}+\mathbf{c})$	2.084(12) 1.858(13)	1.904(14) 1.975(14)	2.013(10) 1.852(10)	2.040(8) (×2)	1.910(9) (×2)
$\pm(\frac{1}{2}\mathbf{a}-\mathbf{c})$	1.899(13) 1.931(13)	1.981(14) 2.041(14)	1.931(10) 1.964(10)	1.930(8) (×2)	2.027(8) (×2)
Mean Mn-O	1.935(11)	1.953(12)	1.931(8)	1.959(6)	1.953(7)
BVS	3.72	3.50	3.73	3.46	3.51

The degree of charge ordering observed via BVS's in transition metal oxides that have undergone symmetry-breaking CO transitions is always much reduced from ideal values. The 25% CO observed here in $Pr_{0.5}Ca_{0.5}MnO_3$ is comparable to that observed (by powder neutron diffraction) in the rocksalt CO manganite $TbBaMn_2O_6$ (20%) (Ref. 22), Fe_3O_4 (20% or 40%) (Ref. 23), $YNiO_3$ (30%) (Ref. 24), and $TbBaFe_2O_5$ (40%) (Ref. 25). No correlation of the magnitude of CO with the magnetic couplings between the charge ordered sites is evident in the latter materials. The magnetic

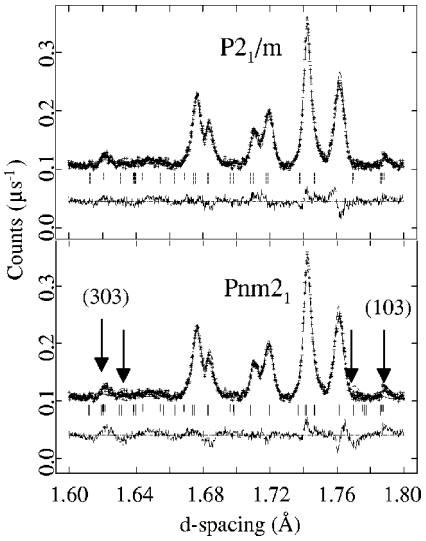

FIG. 2. Part of the observed, calculated, and difference neutron diffraction plots for the fits of $P2_1/m$ and $Pnm2_1$ pseudosymmetry models highlighting the poor fitting of (odd, even, odd) and other superstructure reflections (arrowed) in the latter model.

TABLE II. Refined atomic coordinates for $Pr_{0.5}Ca_{0.5}MnO_3$ at 10 K in space group $P2_1/m$. The lattice parameters are a = 10.8700(2) Å, b = 7.488923(6) Å, c = 5.43499(3) Å, and β = 90.069(1). The isotropic thermal U parameters are Pr/Ca = 0.0079(2) Å^2, Mn = 0.0061(3) Å^2, and O = 0.0084(3) Å^2.

Atom	x	y	z
Pr/Ca1	0.0144(7)	0.25	−0.0081(12)
Pr/Ca2	0.2662(7)	0.25	0.5105(8)
Pr/Ca3	0.5155(7)	0.25	−0.0088(12)
Pr/Ca4	0.7616(7)	0.25	0.4911(7)
Mn1	0.2464(6)	0.0077(6)	0.0084(8)
Mn2a	0	0	0.5
Mn2b	0.5	0	0.5
O1	−0.0079(11)	0.25	0.4361(25)
O2	0.2488(12)	0.25	0.0751(24)
O3	0.4915(11)	0.25	0.4222(24)
O4	0.7407(12)	0.25	0.0661(22)
O5	0.3604(9)	−0.0394(11)	0.2931(14)
O6	−0.1064(7)	0.0476(10)	0.7764(15)
O7	0.8562(7)	−0.0306(12)	0.2624(15)
O8	0.3861(7)	0.0318(12)	0.7917(14)

couplings are all ferromagnetic in Fe_3O_4, all antiferromagnetic in $TbBaFe_2O_5$, and both couplings are present in the CE-type manganite $Pr_{0.5}Ca_{0.5}MnO_3$ and in $YNiO_3$. Hence, the small charge separation in $Pr_{0.5}Ca_{0.5}MnO_3$ and other manganites is a generic feature of symmetry-broken CO transition metal oxides, and is not indicative of specific manganite physics such as Mn^{3+} orbital order.

In conclusion, we find that the two previously reported pseudosymmetry models both yield charge and orbitally ordered descriptions for $Pr_{0.5}Ca_{0.5}MnO_3$ when refined against highly resolved powder neutron and x-ray diffraction data. However, the $P2_1/m$ model, corresponding to Goodenough's original striped CO picture, gives a significantly better fit to neutron superstructure intensities, and so is preferred to the bistriped (or ZPO) $Pnm2_1$ model. These results, in which charge order is evidenced by a full refinement of oxygen atom shifts, complement recent resonant Mn *K* edge x-ray scattering studies that have also favored the striped CO over the ZPO picture.[15,16] The degree of structural charge ordering is only 25% of the expected difference between localized Mn^{3+} and Mn^{4+} states, in common with the CO reduction in other transition metal oxides. This shows that the ordered electrons are not fully localized as simple ions such as Mn^{3+}, although they approximate to this description as evidenced by the observation of OO.

We thank Dr. J.P. Wright, Dr. F. Fauth (ESRF), and Dr. R. Ibberson (ISIS) for assistance with data collection, EPSRC for providing beam time and support for R.J.G., and Professor P.G. Radaelli (ISIS) for useful discussions.

[1] S. Jin, M. McCormack, T. Tiefel, and R. Ramesh, J. Appl. Phys. **76**, 6929 (1994).

[2] M. Uehara, S. Mori, C.H. Chen, and S.-W. Cheong, Nature (London) **399**, 560 (1999).

[3] J.B. Goodenough, Phys. Rev. **100**, 564 (1955).

[4] E.O. Wollan and W.C. Koehler, Phys. Rev. **100**, 545 (1955).

[5] P.G. Radaelli, D.E. Cox, M. Marezio, S.-W. Cheong, P.E. Schiffer, and A.P. Ramirez, Phys. Rev. Lett. **75**, 4488 (1995).

[6] P.G. Radaelli, D.E. Cox, M. Marezio, and S.-W. Cheong, Phys. Rev. B **55**, 3015 (1997).

[7] P.M. Woodward, D.E. Cox, T. Vogt, C.N.R. Rao, and A.K. Cheetham, Chem. Mater. **11**, 3528 (1999).

[8] J. Blasco, J. Garcia, J.M. de Teresa, M.R. Ibarra, J. Perez, P.A. Algarabel, C. Marquina, and C. Ritter, J. Phys.: Condens. Matter **9**, 10 321 (1997).

[9] O. Richard, W. Schuddinck, G. Van Tendeloo, F. Millange, M. Hervieu, V. Caignaert, and B. Raveau, Acta Crystallogr., Sect. A: Found. Crystallogr. **55**, 704 (1999).

[10] A. Daoud-Aladine, J. Rodriguez-Caravajal, L. Pinsard-Gaudart, M.T. Fernandez-Diaz, and A. Revcolevschi, Phys. Rev. Lett. **89**, 097205 (2002); J. Rodriguez-Caravajal, A. Daoud-Aladine, L. Pinsard-Gaudart, M.T. Fernandez-Diaz, and A. Revcolevschi, Physica B **320**, 1 (2002); A. Daoud-Aladine, J. Rodriguez-Caravajal, L. Pinsard-Gaudart, M.T. Fernandez-Diaz, and A. Revcolevschi, Appl. Phys. A: Mater. Sci. Process. **74**, S1758 (2002).

[11] F. Rivadulla, E. Winkler, J.-S. Zhou, and J.B. Goodenough, Phys. Rev. B **66**, 174432 (2002).

[12] D.V. Efremov, J. van den Brink, and D.I. Khomskii, cond-mat/0306651 (unpublished).

[13] A. Yakubovskii, A. Trokiner, S. Verkhovskii, A. Geashenko, and D. Khomskii, Phys. Rev. B **67**, 064414 (2003).

[14] M.v. Zimmermann, C.S. Nelson, J.P. Hill, D. Gibbs, M. Blume, D. Casa, B. Keimer, Y. Murakami, C.-C. Kao, C. Venkataraman, T. Gog, Y. Tomioka, and Y. Tokura, Phys. Rev. B **64**, 195133 (2001).

[15] S. Grenier, J.P. Hill, D. Gibbs, M.v. Zimmermann, C.S. Nelson, V. Kiryukhin, Y. Tokura, Y. Tomioka, D. Casa, T. Gog, and C. Venkataraman, Phys. Rev. B **69**, 134419 (2004).

[16] J. Herrero-Martin, J. Garcca, G. Subias, J. Blanco, and M.C. Sanchez, Phys. Rev. B **70**, 024408 (2004).

[17] J. Garcia, M.C. Sanchez, J. Blasco, G. Subias, and M.G. Proietti, J. Phys.: Condens. Matter **13**, 3243 (2001); J. Garcia and G. Subias, Phys. Rev. B **68**, 127101 (2003); M.v. Zimmermann, S. Grenier, C.S. Nelson, J.P. Hill, D. Gibbs, M. Blume, D. Casa, B. Keimer, Y. Murakami, C.-C. Kao, C. Venkataraman, T. Gog, Y. Tomioka, and Y. Tokura, *ibid.* **68**, 127102 (2003).

[18] J. van den Brink, G. Khaliullin, and D. Khomskii, Phys. Rev. Lett. **83**, 5118 (1999).

[19] A.C. Larson and R.B. Von Dreele, Los Alamos National Laboratory Report No. LAUR 86-748, 1994 (unpublished).

[20] The atomic coordinates were refined independently, initially using Marquardt damping (a scaling of the diagonal elements in the least-squares matrix) to stabilize the refinements. The final $P2_1/m$ refinement was stable without damping whereas the $Pnm2_1$ model required a Marquadt scaling of at least 1.1 for stability, which reflects the acentric symmetry of this space group.

[21] The bond valence sums were calculated using the program VALENCE: I, D. Brown, J. Appl. Crystallogr. **29**, 479 (1996).

[22] A.J. Williams and J.P. Attfield, Phys. Rev. B **66**, 220405 (2002).

[23] J.P. Wright, J.P. Attfield, and P.G. Radaelli, Phys. Rev. B **66**, 214422 (2002).

[24] J.A. Alonso, J.L. Garcia-Munoz, M.T. Fernandez-Diaz, M.A.G. Aranda, M.J. Martinez-Lope, and M.T. Casais, Phys. Rev. Lett. **82**, 3871 (1999).

[25] P. Karen, P. M. Woodward, J. Linden, T. Vogt, A. Studer, and P. Fischer, Phys. Rev. B **64**, 214405 (2001).